



# Investigating the performance of sentinel-2A and Landsat 8 imagery in mapping shoreline changes

George Mitri<sup>1</sup> · Manal Nader<sup>2</sup> · Manale Abou Dagher<sup>2</sup> · Karen Gebrael<sup>1</sup>

Received: 15 April 2019 / Revised: 3 June 2020 / Accepted: 5 June 2020 / Published online: 10 June 2020  
© Springer Nature B.V. 2020

## Abstract

Regular detection and timely monitoring of shoreline evolution are essentially needed in order to identify areas that require further investigation and protection. Possibilities for regular monitoring of shoreline changes are better facilitated now with high-frequency revisit times of Landsat-Sentinel-2 virtual constellation. Accordingly, this study aimed at investigating the performance of Landsat 8 and Sentinel-2A satellite imagery in mapping shoreline changes. The specific objectives were to 1) create reference data of shoreline erosion, accretion and seafilling using very high spatial resolution data, 2) compare the results of shoreline changes by using Landsat 8 and Sentinel-2A imagery respectively, and 3) complete the inventory of shoreline changes between 1962 and 2016. A Quickbird panchromatic imagery (0.6 m) of 2010 was employed in combination with aerial photography (0.5 m) from 1962 for the generation of reference data using a traditional photo-interpretation method. Then, geographic object-based image analysis (GEOBIA) was employed to map changes in the shoreline between 1962 (i.e., reference shoreline) and 2016 using Sentinel-2A (10 m) and Landsat 8 panchromatic band (15 m) imagery, consecutively. The use of Sentinel-2A image provided slightly better accuracy results when compared with those from the Landsat 8 image. Accordingly, an inventory of Lebanese shoreline evolution between 1962 and 2016 was completed using the Sentinel-2A classification results. The combined use of Landsat-Sentinel-2 imagery is expected to generate reliable data records for continuous monitoring of shoreline changes.

**Keywords** Shoreline changes · Landsat-8 panchromatic · Sentinel-2A · Quickbird · Aerial photography, geographic object-based image analysis

## Introduction

A coastal zone is one of the most ecologically, economically and culturally important ecosystem (Brown et al. 2018). It plays a role in supporting local economy based on agricultural, recreational and touristic activities, in addition to fisheries (Sesli 2010). At the same time, a coastal area is a dynamic environment that changes rapidly due to human-caused activities and natural phenomena (Aydin and Uysal 2014; Ahammed and Pandey 2018). On one hand, land reclamation, construction activities, improper land-use practices and

unsustainable recreational and touristic activities are examples of human activities that affect coastal zones. On the other hand, water level changes, shore morphology, variance in wave energies, grain size and sediment composition are natural processes that may induce changes in coastal environment (Sesli 2010; Lorang and Stanford 1993).

Promoting an integrated coastal zone management is based on monitoring shoreline changes (Goncalves and Awange 2017). Shoreline is a component of coastal zone and is defined as “the line of contact between a land and a body of water” (Sesli 2010). A change in shoreline position is a main response to activities and processes that alter and shape surrounding coastal environment (Lo and Gunasiri 2014; Lorang and Stanford 1993). In this context, monitoring changes in shorelines is essential for conservation and management of coastal areas (Bailey and Nowell 1996). Additionally, a shoreline change assessment supports informed decision-making in coastal zone management (Fabbri 1998).

More specifically, erosion and accretion are major phenomena faced by a shoreline change as a result of natural

---

✉ George Mitri  
george.mitri@balamand.edu.lb

<sup>1</sup> Land and Natural Resources Program, Institute of the Environment, University of Balamand, Kelhat, El Koura, Lebanon

<sup>2</sup> Marine and Coastal Resources Program, Institute of the Environment, University of Balamand, El Koura, Lebanon

and human causes. Accordingly, the assessment of these two processes is important while monitoring shoreline changes (Kaliraj et al. 2013; Weitzner 2015). Coastal erosion is defined as removal of sediments from the coast, causing a shoreline retreat, while accretion represents buildup of sediments on a visible portion of the beach (Weitzner 2015). Furthermore, expansion of seashore reclamation activities (i.e., seafilling) constitutes a hazardous factor that affects and disturbs natural ecosystems in coastal zones. Monitoring seafilling, including the creation of new lands from oceans and seas, is also essential while assessing shoreline variations (Jin et al. 2016).

Various approaches have been developed to study changes in shorelines (Suzen and Özhan 2000; Fatallah and Gueddari 2001). These included 1) comparing historical aerial photographs and coastal topographic maps, 2) evaluating erosion, accretion, and seafilling of coastlines, 3) developing models to calculate sediment transport, and 4) identifying hazard prone coastal areas, amongst others.

Traditional techniques for monitoring shoreline changes comprised field assessments and surveys (Quang Tuan et al. 2017; Morton et al. 1993). Field surveys are mainly executed to assess morphological changes along the coast. More specifically, studying the topography near coastline, measuring bathymetry, observing retreat and extent of shoreline and detecting visible impacts of human and natural processes on the coast are accomplished through surveys and field visits (Mahabot et al. 2017). However, field assessments and surveys are considered costly, labor-intensive and time-consuming (Quang Tuan et al. 2017; Boak and Turner 2005).

More recent techniques included the use of aerial photography and satellite remote sensing data. More specifically, remotely sensed data has become an essential tool in numerous types of environmental monitoring (Temiz and Durduran 2016). Consequently, analyzing aerial digital photography and satellite images has become a necessity for coastal studies (Suzen and Özhan 2000). Many studies revealed the importance of using geospatial technologies in estimating shoreline changes through providing researchers with multi-temporal satellites images that cover the entire coastal area (Kaliraj et al. 2013; Nayak 2002; Kumaravel et al. 2013). Moreover, these technologies are able to deliver information within a short period of time while covering large areas.

Mapping shoreline changes using remote sensing data commonly included traditional visual photo-interpretation techniques for spatial feature extraction (Lazaridou 2012; Ghorbani and Pakravan 2013). However, these techniques are highly dependent on the operator capacity in photo-interpretation and require skilled analysts (Schowengerdt 2007). In addition, visual image interpretation is proven to be time-consuming compared to digital interpretation (Ghorbani and Pakravan 2013). Initially, digital analyses of satellite remote sensing data involved pixel-based classification techniques (Blaschke 2010). With the growing

availability of moderate-to-high spatial resolution imagery, fine spatial information and its context could be used to produce more accurate classifications (Mitri and Gitas 2004). Simultaneously, better opportunities for regular assessment and monitoring of shoreline changes exist now due to high-frequency revisit times of satellites, i.e., ~2.9 days, of Landsat-Sentinel-2 virtual constellation (Li and Roy 2017; Tyler et al. 2016). The Multispectral Imager (MSI) on-board Sentinel-2 and the Operational Land Imager (OLI) on-board Landsat-8/9 will enable enhanced regular monitoring within the next 10–15 years (Pahlevan et al. 2017a, 2017b). The 2 to 3-day revisit time will be easily achieved globally when Landsat-9 becomes operational in early 2021 (Pahlevan et al. 2019). Such frequent revisit times are essential to instantaneously capture shoreline dynamics considering cloud coverage.

In this context, the aim of this study was to investigate the performance of Landsat 8 and Sentinel-2A satellite imagery for mapping shoreline changes. The specific objectives were to:

- 1) Create reference data of shoreline erosion, accretion and seafilling using very high spatial resolution data.
- 2) Compare the results of shoreline changes by using Landsat 8 and Sentinel-2A satellite imagery respectively.
- 3) Complete the inventory of shoreline changes between 1962 and 2016.

This work involved the use of Geographic Object-Based Image Analysis (GEOBIA) by addressing the production of meaningful image-objects and the assessment of their characteristics (Blaschke 2010) using both spectral and contextual features of satellite images. The use of GEOBIA provides more meaningful information than traditional pixel-based image analysis (Hidayat et al. 2018) by allowing better distinction among different informational classes.

## Study area and dataset description

The study area consists of the entire Lebanese coastline located in the eastern Mediterranean (Fig. 1). The Lebanese coastline extends over 220 km between Arida in the north and Ras Al-Naqoura in the south (CAS 2008; Badreddine et al. 2018). Approximately 70% of the population in Lebanon lives in the coastal zone, where most of the important cities and economic centers exist (Plan bleu/PNUE 2000; Badreddine et al. 2018). Agricultural activities are present in different locations along the coastal zone (MOE/UNDP, 2011). More than 15 fishing harbors, 4 commercial ports, 3 power plants, a set of sea petroleum pipelines, several industries and 4 major bays (Beirut, Jounieh, Chekka and Akkar) are located along the shoreline (Badreddine et al. 2018). It is important to mention that the Lebanese coastline includes many different natural habitat

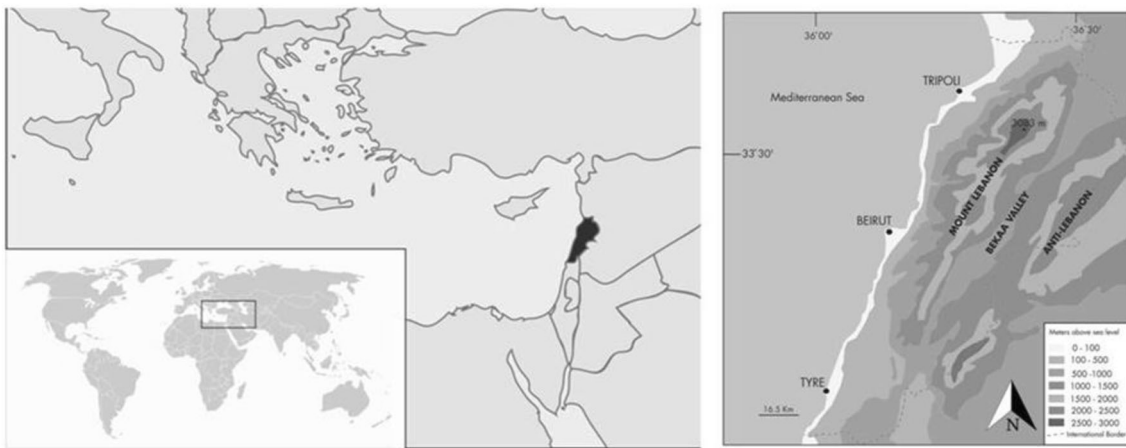


**Fig. 1** Location of the study area

types for endangered fauna and flora (sandy, silty, rocky, neritic, oceanic and coastal habitats) (MOE/UNDP 2011).

In Lebanon, the coast has been experiencing increased anthropogenic pressures such as uncontrolled and illegal urban development, agricultural and industrial runoff, sewage discharge and seashore reclamation (Abou-Dagher et al. 2012; Badreddine et al. 2018). In this context, the detection and monitoring of shoreline evolution are essentially needed in order to identify areas that require further investigation, management and/or protection (Abou-Dagher et al. 2012).

Black and white aerial photographs acquired in the year 1962 with a resolution of 0.5 m were collected, ortho-rectified and mosaicked. A Quickbird panchromatic imagery (0.6 m) of 2010 was also employed. A cloud-free image of Landsat 8 Operational Land Imager (OLI) acquired in 2016 was collected. The image consisted of nine spectral bands with a spatial resolution of 30 m for bands 1 to 7 and 9. The resolution for band 8 (i.e., panchromatic band) was 15 m. The approximate scene size was 170 km north-south by 183 km east-west. In addition, a cloud-free Sentinel-2A image acquired in 2016 was collected. The Sentinel-2A image had a spatial resolution of 30 m and a swath width of 290 km. All remote sensing images were projected at UTM (WGS84-zone 36).

## Methodology

In this study, the adopted methodological approach to investigate the performance of Landsat 8 and Sentinel-2A in mapping changes along the Lebanese shoreline is represented in the following flowchart (Fig. 2).

### Development of reference data

At first, the shorelines of the years 1962 and 2010 were manually digitized using ESRI ArcGIS 9.2 software by tracing and capturing their linear geographic features on the aerial

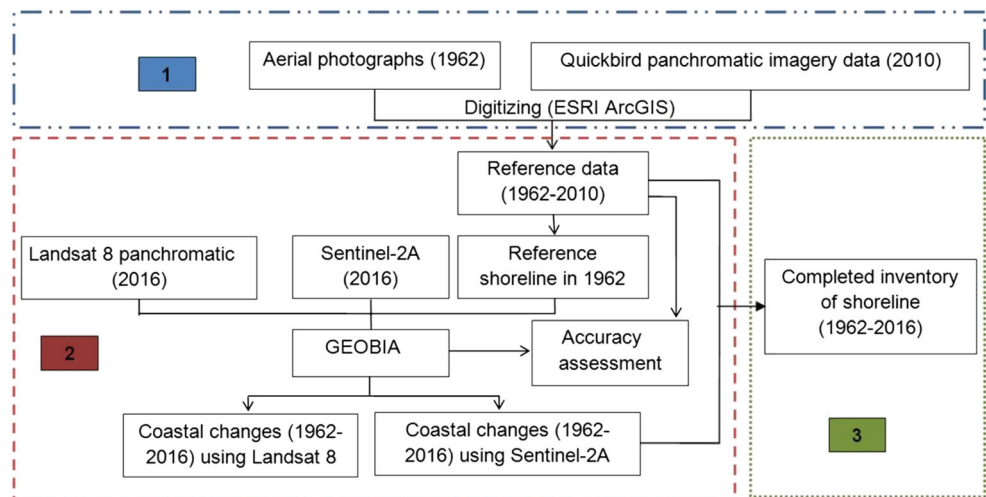
photographs and Quickbird image, respectively. The High Water Mark (HWM), defined as dry/wet line, was adopted as shoreline indicator (Boak and Turner 2005). Then, changes along the shoreline were assessed using the year 1962 as a reference shoreline and 2010 as an initial target year. Assessed changes included erosion, accretion and seafilling. Surfaces were measured as polygon areas and rounding was made at the thousand-level values. The coastlines of 1962 and 2010 were produced in shapefile.

### Geographic object-based image analysis

The assessment of shoreline changes between 1962 and 2016 involved 1) generating image objects or segments for subsequent classification, 2) creating a classification scheme, and 3) mapping the changes in the different land cover categories between the 2 yrs. The GEOBIA approach was adopted by employing the software “eCognition”. One classification model was developed with the use of Sentinel-2A image and another one with the use Landsat 8 panchromatic image.

Each of the Sentinel-2A and Landsat 8 panchromatic images was first segmented and then classified using eCognition (Benz et al. 2004; Gitas et al. 2004). The strategy behind the image segmentation was to create image objects for use in the classification. The segmentation algorithm is essentially a heuristic optimization procedure that minimizes the average heterogeneity of image objects for a given resolution over the whole scene. Weighting between spectral and shape heterogeneity enables adjustment of the segmentation results to the considered application. Segmentation of the Sentinel-2A imagery at the pixel level was generated using an average abstract scale of 10 and equal band weights of the visible and Near Infra-Red (NIR) bands. The composition of homogeneity criteria included the following weights: 10% for shape, 90% for color and 50% for compactness. The segmentation of the Landsat 8 panchromatic layer involved the use of the same abstract scale of 10. Also, the same weights of the

Fig. 2 Methodological approach



composition of homogeneity criteria of shape, color and compactness were adopted.

The classification scheme included the following classes: land in 1962, sea water in 1962, land in 2016, sea water in 2016, land in 1962 converted to water in 2016, and water in 1962 converted to land in 2016. Classifying the image objects to map land cover changes between the 2 yrs involved the use of the reference shoreline of 1962 as a thematic layer and mean spectral layer features of the Sentinel-2A imagery (including visible and NIR bands) and the Landsat-8 panchromatic band. Subsequently, contextual features (i.e., relationship among classified objects) were employed for change detection mapping.

### Comparison of classification results and development of the inventory

In order to compare and evaluate the classification results between those of the Sentinel-2A imagery and the Landsat 8 panchromatic band, a spatial analysis using ArcGIS was conducted. This included the production of intersection layers between “reference data” of the 1962–2010 and the change detection maps derived from the use of Sentinel-2A imagery and Landsat 8 panchromatic image, respectively. Non-intersected polygons were excluded in the analysis given that relatively small changes across the shoreline might have happened between 2010 and 2016, the dates in which the satellite images were acquired. Finally, an inventory of shoreline changes between 1962 and 2016 was produced using the image classification results of highest accuracy.

### Results and discussion

Initially, surfaces of erosion, accretion and seafilling were assessed and interpreted by overlaying the 1962 and 2010

shorelines (Table 1). It is worth mentioning that the calculated shoreline length was 297.87 km in 1962 and 370.92 km in 2010. The produced “reference data” was used for evaluating the classification performance of GEOBIA in each of the two cases of employing satellite imagery of 2016.

The applied method for generating reference data could be affected by two sources of errors, namely errors caused by the data sources and errors caused by the interpretation and the measurements (Moore 2000). More specifically, possible causes of errors include radial distortion, photo shrink or stretch of data (i.e., aerial photography). The ortho-rectification of the aerial photography resulted in a total Root-Mean-Square (RMS) error value of 2.8. As for the interpretation, errors could

Table 1 Evolution of the Lebanese shoreline between 1962 and 2010 (reference data)

Type of change between 1962 and 2010			
Cazas	Erosion (m <sup>2</sup> )	Accretion (m <sup>2</sup> )	Seafilling (m <sup>2</sup> )
Akkar	786,748	5001	37,862
Minieh -Dannieh	154,948	0	68,898
Tripoli	37,394	1874	1,110,686
Koura	10,149	0	236,176
Batroun	119,642	33,417	278,881
Jbeil	9936	0	117,548
Kesrouane	1625	9313	863,328
El-Maten	0	0	2,108,456
Beirut	4483	46,368	2,086,842
Baabda	5406	15,143	648,234
Aley	37,457	1242	294,182
Chouf	305,978	12,599	188,744
Saida	304,036	25,710	137,254
Sour	827,401	6726	111,828
<b>Total area (m<sup>2</sup>)</b>	<b>2,605,203</b>	<b>157,394</b>	<b>8,288,918</b>

occur due to seasonal changes that result in the movement of the dry/wet line. Such errors are reduced by making sure that most images are taken during the same season, the best being the summer season. Additionally, working with different resolutions/characteristics could lead to a misinterpretation of the shoreline position. Yet, shaded areas resulting from cliffs on seaside can in some cases mask some parts of the shoreline.

The classification of the satellite imagery showed results (i.e., classified polygons) of two main classes, namely, loss of land to sea water (i.e., erosion) and gain of land in sea water (i.e., accretion and seafilling). The evaluation of the classification results involved comparing the common areas between the reference data and the polygons resulting from image classification of Sentinel-2A and Landsat-8, respectively (Table 2).

The overall classification accuracy of Sentinel-2A imagery (i.e., 99.5%) was slightly higher than that of Landsat-8 panchromatic band (99.27%). The main difference in mapping changes was at the level of user’s accuracy for mapping loss of land using Landsat-8 panchromatic (i.e., 95.5%) and Sentinel-2A imagery (i.e., 99.5%). This could be explained by the improved ability to segment and classify small geographic variations across the land-water interface when using higher spatial resolution data and multi-spectral information from the Sentinel-2A image.

Considering results from similar studies, Forkuor et al. (2018) found that classification of Sentinel-2A bands common to Landsat-8 produced an overall accuracy that was 4% better than that of Landsat 8 when mapping land use and land cover (LULC). The improved discrimination of LULC classes was mostly attributed to the Sentinel-2A red-edge bands. Yet, the performance of using Sentinel-2A bands versus Landsat 8 panchromatic band of 15 m resolution needs to be also investigated. In this context, Labib and Harris (2018) noted that Sentinel-2A image performed better in classifying Green Infrastructure (GI) when compared to the use of Landsat 8 panchromatic image using GEOBIA. The former resulted in 71.41% of overall accuracy while the latter resulted in an overall accuracy of 67.85% (i.e., -3.56%) despite the 5-m variation in spatial resolution between the two images. In comparison to Landsat 8 (i.e., after pan-sharpening), classifications of Sentinel 2-A were smoother (i.e., result of the 5-m

difference in pixel size between the two images). More specifically, it was found that water bodies were under- or over-classified using the panchromatic Landsat 8 while feature extraction and delineation of object boundary were highly accurate in the case of Sentinel-2A results. In the context of this work, the slight difference between the two overall accuracies is mostly explained by the conducted discrimination between two classes only (i.e., namely water and land). However, the higher differences between overall accuracies in the other studies (Forkuor et al. 2018; Labib and Harris 2018) were mostly attributed to discriminating among many other different LULC classes. This accounted for significantly improved distinction between specific classes (e.g., vegetation and built-up among others) in comparison to other classes.

Further investigation of the results indicated how the shape, color and compactness criteria used in the segmentation process helped in producing spatially homogeneous objects in strongly textured data (Fig. 3). Objects (i.e., segments) developed for Sentinel-2A image properly fitted with water bodies. Segments clearly distinguished objects with clear boundaries. In contrast, some of the segments produced from the Landsat 8 panchromatic image did not homogeneously represent a whole object. Labib and Harris (2018) argued that the spatial resolution of Sentinel-2A parameters positively influenced the image segmentation process.

Based on segmentation, specific spectral information (i.e., mean values of spectral bands) and contextual information (i.e., spatial relationship of image objects) were made available for classification. In turn, based on classification of image objects using membership functions of contextual and spectral features, desired classes of interest were extracted in a step-wise approach.

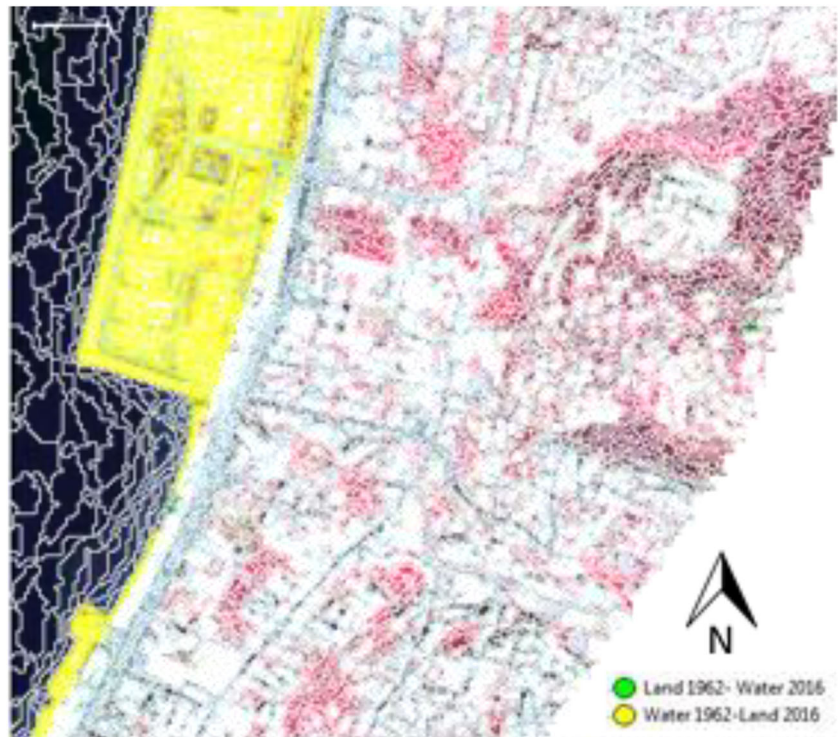
Consequently, the image classification results of the Sentinel-2A data (1962–2016) were compared to the reference data (1962–2010) in order to complete the inventory of shoreline evolution between 1962 and 2016 across the different Cazas (i.e., administrative districts of Lebanon). Land areas gained in seawater between 2010 and 2016 were further segregated into accretion and seafilling based on photo-interpretation. The results were summarized in Table 3 and Fig. 4.

More specifically, it was found that the area of seafilling in reference data amounted to 76.58% of seafilling between

**Table 2** A comparative evaluation of the image classification results

	Landsat-8 panchromatic	Sentinel-2A (visible and near infra-red)
Producer’s accuracy (%)		
Loss	99.37	99.14
Gain	99.26	99.89
User’s accuracy (%)		
Loss	95.4	99.5
Gain	99.9	99.82
Overall accuracy (%)	<b>99.27</b>	<b>99.5</b>

**Fig. 3** A subset of segmented and classified Sentinel-2A image



1962 and 2016 using the Sentinel-2A imagery. This difference is mostly explained by the various seafilling activities which took place along the El-Maten district between 2010 and 2016. In addition, the area of erosion in reference data was higher by 26% in comparison to the area of erosion between 1962 and 2016, while the area of accretion in reference data

represented 41.22% of accretion between 1962 and 2016. On one side, the increasing area of accretion between 2010 and 2016 significantly contributed to decreasing the area of erosion between 1962 and 2016. On the other side, an accretion area (i.e., representing 4.18% of the total seafilling between 1962 and 2016) could be mistakenly classified as seafilling.

**Table 3** Sentinel-2A shoreline data for 2016

Type of change between 1962 and 2016			
Cazas (i.e., districts)	Erosion (m <sup>2</sup> )	Accretion (m <sup>2</sup> )	Seafilling (m <sup>2</sup> )
Akkar	703,831	4900	56,650
Minieh –Dannieh	178,069	1100	86,970
Tripoli	15,400	4300	1,675,731
El-Koura	19,050	400	468,069
Batroun	115,250	35,800	367,737
Jbeil	14,550	18,367	173,915
Kesrouane	1300	46,984	1,050,206
El-Maten	0	0	2,279,432
Beirut	0	84,350	2,271,323
Baabda	0	18,550	781,360
Aley	20,800	0	458,350
Chouf	224,065	18,300	282,900
Saida	199,966	100,819	704,856
Sour	435,224	47,895	165,964
<b>Total</b>	<b>1,927,504</b>	<b>381,765</b>	<b>10,823,462</b>

The shoreline inventory of 1962–2016 (Fig. 5) showed that the largest area of erosion was in Akkar (703,831 m<sup>2</sup>), followed by Sour (435,224 m<sup>2</sup>) and Chouf (224,065 m<sup>2</sup>). As for accretion, the largest area was in Saida (100,819 m<sup>2</sup>), followed by Beirut (84,350 m<sup>2</sup>), Sour (47,895 m<sup>2</sup>) and Kesrouane (46,984 m<sup>2</sup>). Moreover, the largest seafilling areas were found in El-Maten (2,279,432 m<sup>2</sup>), Beirut (2,271,323 m<sup>2</sup>), Tripoli (1,675,731 m<sup>2</sup>) and Kesrouane (1,050,206 m<sup>2</sup>). Erosion,

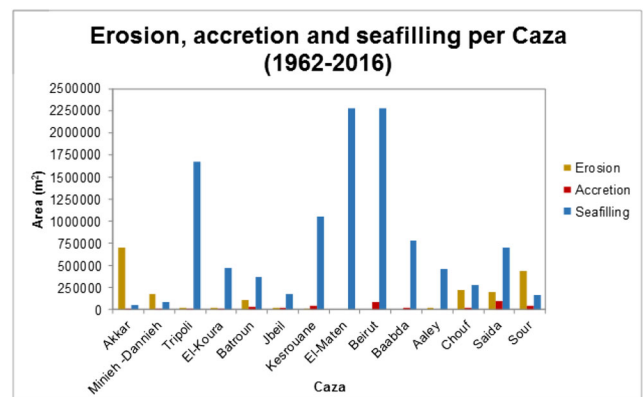
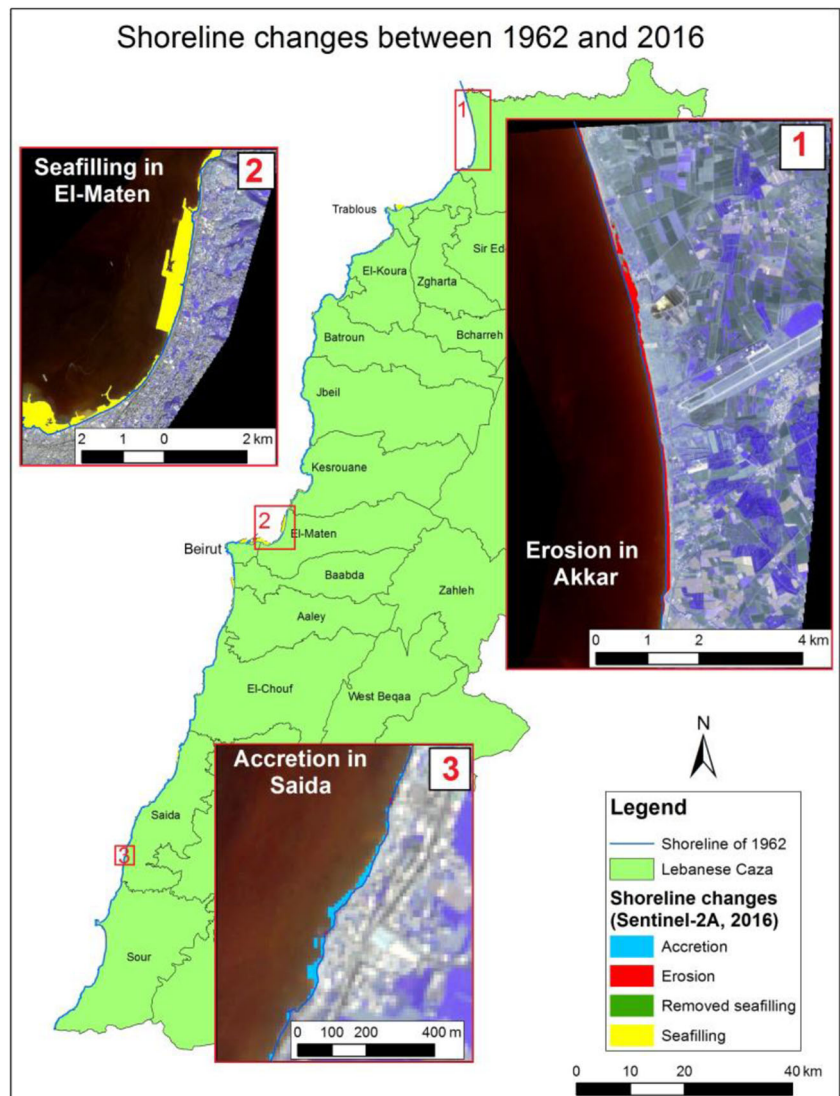


**Fig. 4** The total area (in m<sup>2</sup>) of erosion, accretion and seafilling per Caza (i.e., districts) (1962–2016)

**Fig. 5** Subsets of shoreline changes between 1962 and 2016



accretion and seafilling are expected to significantly affect coastal dynamics and morphology at different locations along the shoreline. Further focused and site-specific investigations to assess impact on coastal and marine habitats will need to be conducted accordingly.

Overall, the combined use of GEOBIA and satellite images of Landsat-8 and Sentinel-2A provided satisfactory results in mapping gains and losses of land along the shoreline. This is considered as an essential step towards using an operational tool for identifying coastal areas of possible concerns, therefore requiring further investigation.

### Conclusions

Understanding the causes of coastal changes as well as continuously monitoring changes of sand/pebble beaches, coastal currents and wave profiles (i.e., particularly around eroded

and seafilled areas) are essential steps towards designing and adopting proper mitigation actions.

In this context, this study aimed at investigating changes along the Lebanese shoreline using object-based image analysis of Sentinel-2A and Landsat-8. Although the classification of the two images resulted in close mapping accuracies, the use of Sentinel-2A imagery provided slightly better classification reliability. Yet, both images showed satisfactory results in mapping shoreline changes. This justifies the beneficial complementary use of Landsat-8 panchromatic band and Sentinel-2A imagery in GEOBIA for operational mapping and monitoring of shorelines. Recognizing the slight differences in their spectral and spatial sampling, the combined use of near-simultaneous Landsat-8 and Sentinel-2A satellite products is expected to open opportunities for capturing the dynamics of shoreline at rates that have never been possible before. This is expected to generate a seamless data record for local, national and even global shoreline monitoring.

As GEOBIA worked well with Sentinel-2A and Landsat 8 images, future work involves further improvement. This includes investigating different optimizations of the segmentation process and additional investigation of rule-based classification. In turn, this is expected to support the future automation of the mapping procedure, therefore facilitating transferability and replicability of the image classification models.

## References

- Abou-Dagher M, Nader M and El Indary S (2012) Evolution of the coast of North Lebanon from 1962–2007: mapping changes for the identification of hotspots and for future management interventions. Fourth Symposium "Monitoring of Mediterranean coastal areas: problems and measurement techniques" - Livorno (Italy) 12–13-14
- Ahamed KKB, Pandey AC (2018) Shoreline morphology changes along the eastern coast of India, Andhra Pradesh by using geospatial technology. *J Coast Conserv* 23(2):331–353. <https://doi.org/10.1007/s11852-018-0662-5>
- Aydn M, Uysal M (2014) Risk assessment of coastal erosion of Karasu coast in Black Sea. *J Coast Conserv* 18(6):673–682. <https://doi.org/10.1007/s11852-014-0343-y>
- Badreddine A, Saab MAA, Gianni F, Ballesteros E, Mangialajo L (2018) First assessment of the ecological status in the Levant Basin: application of the CARLIT index along the Lebanese coastline. *Ecol Indic* 85:37–47. <https://doi.org/10.1016/j.ecolind.2017.10.006>
- Bailey B, Nowell D (1996) Techniques for monitoring coastal change: a review and case study. *Ocean Coast Manag* 32(2):85–95. [https://doi.org/10.1016/S0964-5691\(96\)00058-0](https://doi.org/10.1016/S0964-5691(96)00058-0)
- Benz U, Hofmann P, Willhauck G, Lingenfelder I, Heynen M (2004) Multi-resolution, object-oriented fuzzy analysis of remote sensing data for GIS-ready information. *ISPRS J Photogramm Remote Sens* 58(3–4):239–258. <https://doi.org/10.1016/j.isprsjprs.2003.10.002>
- Blaschke T (2010) Object based image analysis for remote sensing. *Int J Photogram Remote Sensing* 65(1):2–16. <https://doi.org/10.1016/j.isprsjprs.2009.06.004>
- Boak EH, Turner I (2005) Shoreline definition and detection: a review. *J Coast Res* 21(4):688–703. <https://doi.org/10.2112/03-0071.1>
- Brown EJ, Vasconcelos RP, Wennhage H, Bergstrom U, Stottrup JG, Van de Wolfshaar K, Millisenda G, Colloca F, Le Pape O (2018) Conflicts in the coastal zone: a rapid assessment of human impacts on commercially important fish species utilizing coastal habitat. *ICES J Mar Sci* 75(4):1203–1213. <https://doi.org/10.1093/icesjms/lsx237>
- CAS (2008) Morphology, Climatology, Hydrology, Vegetation and Environment. In: Statistical Yearbook 2008. Central Administration of Statistics, Beirut
- Fabbri KP (1998) A methodology for supporting decision making in integrated coastal zone management. *Ocean & Coastal Management* 39(1–2):51–62. [https://doi.org/10.1016/S0964-5691\(98\)00013-1](https://doi.org/10.1016/S0964-5691(98)00013-1)
- Fatallah S, Gueddari M (2001) Sedimentary processes and shoreline changes along the Sousse coast, eastern Tunisia. In: Özhan E (Ed.) Proc. of the fifth international conference on the Mediterranean coastal environment, MEDCOAST 01, MEDCOAST Secretariat, Middle East Technical University, Ankara, Turkey, 3: 1457–1466
- Forkuor G, Dimobe K, Serme I, Tondoh JE (2018) Landsat-8 vs. Sentinel-2: examining the added value of sentinel-2's red-edge bands to land-use and land-cover mapping in Burkina Faso. *GISci Remote Sensing* 55(3):331–354. <https://doi.org/10.1080/15481603.2017.1370169>
- Ghorbani A, Pakaravan M (2013) Land use mapping using visual vs. digital image interpretation of TM and Google earth derived imagery in Shrivani-Darasi watershed (northwest of Iran). *Eur J Experiment Biol* 3(1):576–582
- Gitas I, Mitri G, Ventura G (2004) Object-based image classification for burned area mapping of Creus cape, Spain, using NOAAVHRR imagery. *Remote Sens Environ* 92(3):409–413. <https://doi.org/10.1016/j.rse.2004.06.006>
- Goncalves RM, Awange JL (2017) Three Most widely used GNSS-based shoreline monitoring methods to support integrated coastal zone management policies. *J Surv Eng* 143(3):05017003. [https://doi.org/10.1061/\(ASCE\)SU.1943-5428.0000219](https://doi.org/10.1061/(ASCE)SU.1943-5428.0000219)
- Hidayat F, Ruiastuti A, Purwonon N (2018) GEOBIA an (Geographic) Object-Based Image Analysis for coastal mapping in Indonesia: A Review IOP. Conf Ser: Earth Environ Sci 162:012039
- Jin W, Yang W, Sun T, Yang Z, Li M (2016) Effects of seashore reclamation activities on the health of wetland ecosystems: a case study in the Yellow River Delta, China. *Ocean Coastal Manag* 123:44–52. <https://doi.org/10.1016/j.ocecoaman.2016.01.013>
- Kaliraj S, Chandrasekar N, Magesh NS (2013) Evaluation of coastal erosion and accretion processes along the southwest coast of Kanyakumari, Tamil Nadu using geospatial techniques. *Arab J Geosci* 8(1):239–253. <https://doi.org/10.1007/s12517-013-1216-7>
- Kumaravel S, Ramkumar T, Gurunanam B, Suresh M, Dharanirajam K (2013) An application of remote sensing and GIS based shoreline change studies – a case study in the Cuddalore District, East Coast of Tamilnadu, South India. *Int J Innov Technol Explor Eng* 2(4):211–215
- Labib SM, Harris A (2018) The potentials of Sentinel-2 and LandSat-8 data in green infrastructure extraction, using object based image analysis (OBIA) method. *Eur J Remote Sensing* 51(1):231–240. <https://doi.org/10.1080/22797254.2017.1419441>
- Lazaridou MA (2012) Image interpretation of coastal areas. International Archives of the Photogrammetry, Remote Sensing and Spatial Information Sciences. International Archives of the Photogrammetry, Remote Sensing and Spatial Information Sciences Volume XXXIX-B8, XXII ISPRS Congress (25 August–01 September 2012), Melbourne, Australia
- Li J, Roy DP (2017) A global analysis of sentinel-2A, sentinel-2B and Landsat-8 data revisit intervals and implications for terrestrial monitoring. *Remote Sens* 9(9):902. <https://doi.org/10.3390/rs9090902>
- Lo KFA, Gunasiri CWD (2014) Impact of coastal land use change on shoreline dynamics in Yunlin county, Taiwan. *Environments* 1: 124–136. <https://doi.org/10.3390/environments1020124>
- Lorang MS, Stanford JA (1993) Variability of shoreline erosion and accretion within a beach compartment of flathead Lake, Montana. *Limnol Oceanogr* 38(8):1783–1795. <https://doi.org/10.4319/lo.1993.38.8.1783>
- Mahabot MM, Jaud M, Gwenaelle P, Le Dantec N, Troadec R, Suanes S, Delacourt C (2017) The basics for a permanent observatory of shoreline evolution in tropical environments; lessons from back-reef beaches in La Reunion Island. *Compt Rendus Geosci* 349(6–7):330–340. <https://doi.org/10.1016/j.crte.2017.09.010>
- Mitri G, Gitas I (2004) A performance evaluation of a burned area object-based classification model when applied to topographically and non-topographically corrected TM imagery. *Int J Remote Sens* 25(14): 2863–2870. <https://doi.org/10.1080/01431160410001688321>
- MOE/UNDP (2011) Climate change vulnerability and adaptation, coastal zones. Lebanon's Second National Communication. Ministry of Environment, Beirut
- Moore L (2000) Shoreline mapping techniques. *J Coast Res* 16(1):111–124
- Morton RA, Leach MP, Paine JG, Cardoza MA (1993) Monitoring beach changes using GPS surveying techniques. *J Coast Res* 9(3):702–720. <http://www.jstor.org/stable/4298124>



- Nayak SR (2002) Use of satellite data in coastal mapping. *Ind Cartograph* 22:147–175
- Pahlevan N, Sarkar S, Franz B, Balasubramanian S, He J (2017a) Sentinel-2 multispectral instrument (MSI) data processing for aquatic science applications: demonstrations and validations. *Remote Sens Environ* 201:47–56. <https://doi.org/10.1016/j.rse.2017.08.033>
- Pahlevan N, Schott J, Franz B, Zibordi G, Markham B, Bailey S, Schaaf C, Ondrusek M, Greb S, Strait C (2017b) Landsat 8 remote sensing reflectance (R<sub>rs</sub>) products: evaluations, intercomparisons, and enhancements. *Remote Sens Environ* 190:289–301. <https://doi.org/10.1016/j.rse.2016.12.030>
- Pahlevan N, Chittimalli S, Balasubramanian S, Vellucchie V (2019) Sentinel-2/Landsat-8 product consistency and implications for monitoring aquatic systems. *Remote Sens Environ* 220:19–29. <https://doi.org/10.1016/j.rse.2018.10.027>
- Plan bleu/PNUE (2000) Profile des pays méditerranéens, Liban: Enjeux et politiques d'environnement et de développement durable. Plan Bleu: Sophia-Antipolis. *Remote Sensing for Managing Coastal Areas and River Basins*, Ispra
- Quang Tuan N, Cong Tin H, Quang Doc L, Tuan T (2017) Historical monitoring of shoreline changes in the Cua Dai estuary, Central Vietnam using multi-temporal remote sensing data. *Geosciences* 7(3). <https://doi.org/10.3390/geosciences7030072>
- Schowengerdt R (2007) The nature of remote sensing. In: *Remote sensing, 3<sup>rd</sup> edn. Models and Methods for Image Processing*, pp 1–44
- Sesli FA (2010) Mapping and monitoring temporal changes for coastline and coastal area by using aerial data images and digital photogrammetry: a case study from Samsun. *Int J Phys Sci* 5(10):1567–1575. <https://doi.org/10.1007/s10661-008-0366-7>
- Süzen L, Özhan E (2000) Monitoring of shoreline changes around Yesilirmak Delta by using remote sensing. *International MEDCOAST Conference on the Use of Remote Sensing for Managing Coastal Areas and River Basins*, Ispra
- Temiz F, Durduran S (2016) Monitoring coastline change using remote sensing and GIS technology: a case study of Acıgöl Lake, Turkey. *IOP Conf. Series: Earth and Environmental Science*
- Tyler AN, Hunter PD, Spyarakos E, Groom S, Constantinescu AM, Kitchen J (2016) Developments in earth observation for the assessment and monitoring of inland, transitional, coastal and shelf-sea waters. *Sci Total Environ* 572:1307–1321. <https://doi.org/10.1016/j.scitotenv.2016.01.020>
- Weitzner H (2015) Coastal processes and causes of shoreline erosion and accretion. New York Sea Grant. <https://seagrant.sunysb.edu/glcoastal/pdfs/ShorelineErosion.pdf>. Accessed 15 March 2019

**Publisher's note** Springer Nature remains neutral with regard to jurisdictional claims in published maps and institutional affiliations.